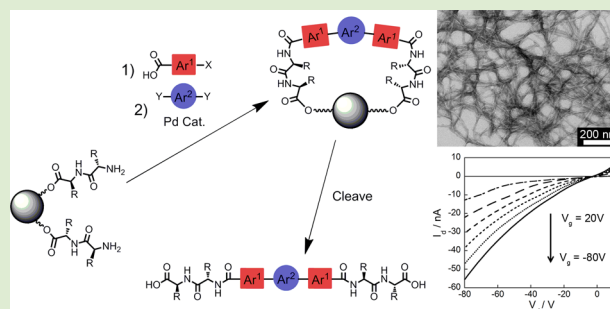


Peptide-Based Supramolecular Semiconductor Nanomaterials via Pd-Catalyzed Solid-Phase "Dimerizations"

Allix M. Sanders,[†] Thomas J. Dawidczyk,[‡] Howard E. Katz,^{†,‡} and John D. Tovar^{*,†,‡,§}[†]Department of Chemistry, [‡]Department of Materials Science and Engineering, [§]Institute for NanoBioTechnology, Johns Hopkins University, 3400 North Charles Street, Baltimore, Maryland 21218, United States

Supporting Information

ABSTRACT: We report a streamlined method for the synthesis of peptides embedded with complex and easily variable π -conjugated oligomeric subunits from commercially available precursors. These modified peptides self-assemble under aqueous conditions to form one-dimensional nanomaterials containing networks of π -stacked conduits, despite the inclusion of π -conjugated oligomers with quadrupoles extended over larger areas. The procedure has circumvented solubility and other synthetic issues to allow for the facile formation of a diverse library of bioelectronic nanomaterials, including a complex sexithiophene-containing peptide whose nanostructures display gate-induced conductivity within field effect transistors.



Peptide-based π -electron scaffolds offer a unique ability to encourage exciton coupling among π -conjugated subunits in aqueous environments.^{1–4} These scaffolds promote delocalized electronic states among the component conjugated oligomers and, due to their peptidic nature, offer an enticing segue into biological investigations. Current state of the art consists of molecular structures such as synthetic polypeptides or genetically modified α -helical proteins that position π -conjugated oligomers with defined spatial orientations, thereby leading to collective electronic delocalization among otherwise isolated electronic units.² Likewise, π -electron peptidic materials can be directed to aggregate into nanostructured materials with tube or tape-like morphologies.^{3,4} Many of the common synthetic approaches to install the requisite π -electron units involve solution-phase reactions between the π -conjugated segments and the peptide fragments, using reactive functional groups such as amines or carboxylic acids (for amide bond formation) or alkynes (for Huisgen-type cycloadditions). These examples, however, require the up-front chemical synthesis of the conjugated oligomer of interest appended with the necessary reactive groups to allow for ligation onto or within the peptide framework, thus, posing challenges for mutual peptide/chromophore solubility and for final construct purification.

We recently reported an alternative synthetic strategy that keeps the peptides bound to solid supports during the installation of the π -electron segments via site–site double amidation between immobilized peptides and π -conjugated diacids.⁴ This approach still requires the synthesis of the diacid components, and the solubilities of the critical π -electron segments become problematic as the conjugated oligomer is made longer.

To circumvent these problems, we sought to utilize the power of Pd-mediated cross-coupling as a tool to provide diverse π -conjugated systems that incorporate several different aryl–aryl linkages embedded within self-assembling peptide architectures through the union of small, soluble components, many of which are readily available commercially. This remarkably facile approach in principle eliminates the need for lengthy solution-phase purification of synthesis intermediates. The procedure has also evaded problematic solubility issues in order to access conjugated units up to sexithiophene, which to our knowledge is the longest peptide-embedded oligothiophene to be rendered water-soluble yet still able to self-assemble into semiconductive 1-D nanostructures. Although transition metal-mediated chemistries have been utilized on solid supports,⁵ we present a unique example of solid-phase palladium-catalyzed cross-coupling dimerizations. This approach allows for the facile preparation of aqueous self-assembling systems that encourage the intermolecular electronic delocalization among tunable π -electron segments within well-defined 1-D nanostructures.

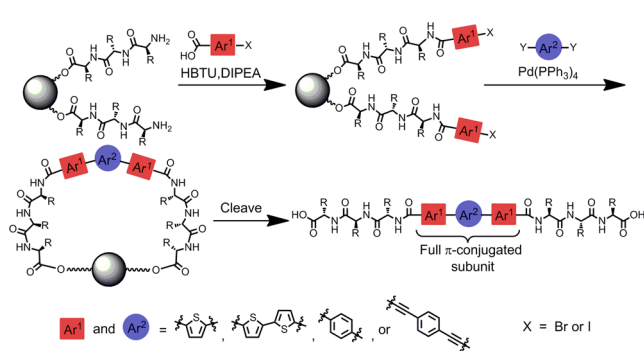
The synthetic strategy is illustrated in Scheme 1. A small oligopeptide, immobilized on a resin bead, is synthesized via standard Fmoc solid phase peptide synthesis (SPPS). A portion of the π -conjugated subunit (Ar^1 = thiophene, bithiophene, or phenyl), differentially substituted with a halide (Br or I) and a carboxylic acid group (e.g., 4-iodobenzoic acid), is added to the resin under standard amino acid coupling conditions. *N*-Acylation of the amine termini of the peptide fragments with

Received: September 4, 2012

Accepted: October 25, 2012

Published: October 30, 2012

Scheme 1. Solid-Phase Palladium Catalyzed Cross-Coupling Procedure



the in situ activated carboxylic acid moiety on Ar^1 immobilizes the aryl halide on the solid phase. A second arene (Ar^2), disubstituted with mutually reactive functionality for transmetalation under palladium catalysis, is introduced to the resin so that site–site cross coupling can occur. Using either a distannylated Ar^2 ($Y = \text{SnBu}_3$) under Stille conditions, a diboronic acid ($Y = \text{B}(\text{OH})_2$) under Suzuki conditions, or diethynyl benzene ($Y = \text{C}\equiv\text{CH}$) under Sonogashira conditions, with $\text{Pd}(\text{PPh}_3)_4$ as the catalyst, coupling between the disubstituted Ar^2 segment and two aryl halides takes place. Upon cleavage and isolation, peptides embedded with Ar^1 – Ar^2 – Ar^1 π -conjugated oligomeric subunits are obtained.

The method has proven versatile in the straightforward synthesis of a wide range of π -conjugated peptides (Table 1). Obtaining the same peptides using classical routes would have required the upfront preparation of requisite amino acid or diacid oligomers by way of several synthetic manipulations (cross-couplings, lithiations, chromatography, crystallizations, etc.), all on sparingly soluble products. With this method, utilization of thiophene-based aryl components under Stille reaction conditions allowed for the formation of oligothiophene-containing peptides ranging from terthiophene (**1**) to sexithiophene (**4**), directly from simple mono- and bithiophene building blocks. Furthermore, commercially available 4-iodobenzoic acid and 1,4-benzene diboronic acid were employed under Suzuki cross-coupling conditions to obtain terphenyl peptide **6**. The method also provides mixed aromatic systems consisting of alternating thiophene and phenyl rings using either Stille (**5**) or Suzuki (**7**) conditions. Sonogashira cross-coupling conditions, utilizing 4-iodobenzoic acid and 1,4-diethynyl benzene, provided oligophenylene-ethynylene (OPE3) peptide **8**. The initial synthesis attempt resulted in a partially hydrogenated alkyne product, as determined by NMR, potentially due to a small amount of remaining palladium catalyst and the presence of triisopropylsilane during cleavage.⁶ To remedy this, the silane was eliminated from the cleavage cocktail, and the partial hydrogenation side-reaction was no longer seen. The fairly sensitive OPE3 chromophore remained intact, despite the harsh acidic cleavage conditions, thereby suggesting that other comparably sensitive π -electron units will tolerate the cleavage chemistry. It is also conceivable to use a resin support that can be cleaved using less aggressive acidic conditions.

The peptide sequences were chosen mainly for solubility reasons. For instance, due to the tendency of intermolecular aggregation of longer oligothiophenes, sequences containing more ionizable amino acids were selected to allow for aqueous solubility with minimal aggregation under basic pH (e.g., **3** and

Table 1. Library of π -Conjugated Peptides

$\text{HO}-\text{Ar}^1-\text{X}$	$Y-\text{Ar}^2-Y$	method	product ^e
		Stille ^d	DFAG-NH-(S) ₁ -NH-GAFD (1)
		Stille ^d	DFAG-NH-(S) ₂ -NH-GAFD (2)
		Stille ^d	DADGG-NH-(S) ₃ -NH-GGDAD (3)
		Stille ^d	DADDG-NH-(S) ₄ -NH-GDDAD (4)
		Stille ^d	VEVAG-NH-(S) ₅ -NH-GAVEV (5)
		Suzuki ^f	VEVAG-NH-(Ph) ₃ -NH-GAVEV (6)
		Suzuki ^f	VEVAG-NH-(S) ₂ -Ph-(S) ₂ -NH-GAVEV (7)
		Sonogashira ^g	DFAG-NH-(Ph) ₂ -C≡C-Ph-C≡C-Ph-NH-GAFD (8)

^aAll equivalents were determined with respect to the amino acid loading of the peptide resin that was used (0.8–0.67 mmol/g).

^bCleavage of the peptide from the resin was performed by treating the resin to a 10:0.25:0.25 cocktail of TFA/TIPS/ H_2O for 3 h. ^cProduct yields after cleavage and dialysis were 25–54% and after HPLC purification were 2.5–12% (see SI). ^dStille reaction conditions utilized 0.5 equiv of the distannylated arene and 4 mol % $\text{Pd}(\text{PPh}_3)_4$ in DMF for 16–21 h at 80 °C. ^eSuzuki reaction conditions utilized 0.55 equiv of benzene-1,4-diboronic acid, 4 mol % $\text{Pd}(\text{PPh}_3)_4$, K_2CO_3 (8 equiv), in DMF/ H_2O (4:1), for 20–27 h at 80 °C. ^fSonogashira reaction conditions utilized 0.55 equiv of 1,4-diethynyl benzene, 5 mol % $\text{Pd}(\text{PPh}_3)_4$, 10 mol % CuI , in DMF for 18 h at RT. TIPS was omitted from cleavage cocktail.

4). Under these conditions, the carboxylic acid groups are deprotonated, thus exploiting charge repulsion to prevent intermolecular association. The UV–vis absorption spectra of **1–4** in water at pH 8 (Figure 1) showed an increasingly red-shifted λ_{max} from 392 nm (**1**) to 447 nm (**4**), owing to the

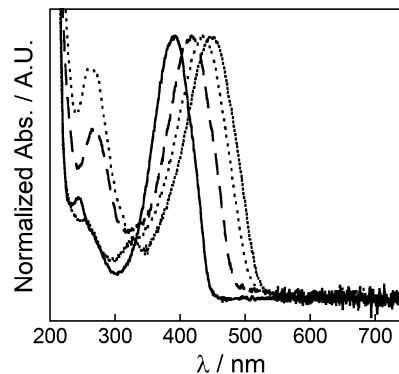


Figure 1. Normalized UV–vis spectra of unassembled **1** (—), **2** (---), **3** (⋯⋯), and **4** (—⋯) in pH 8 water.

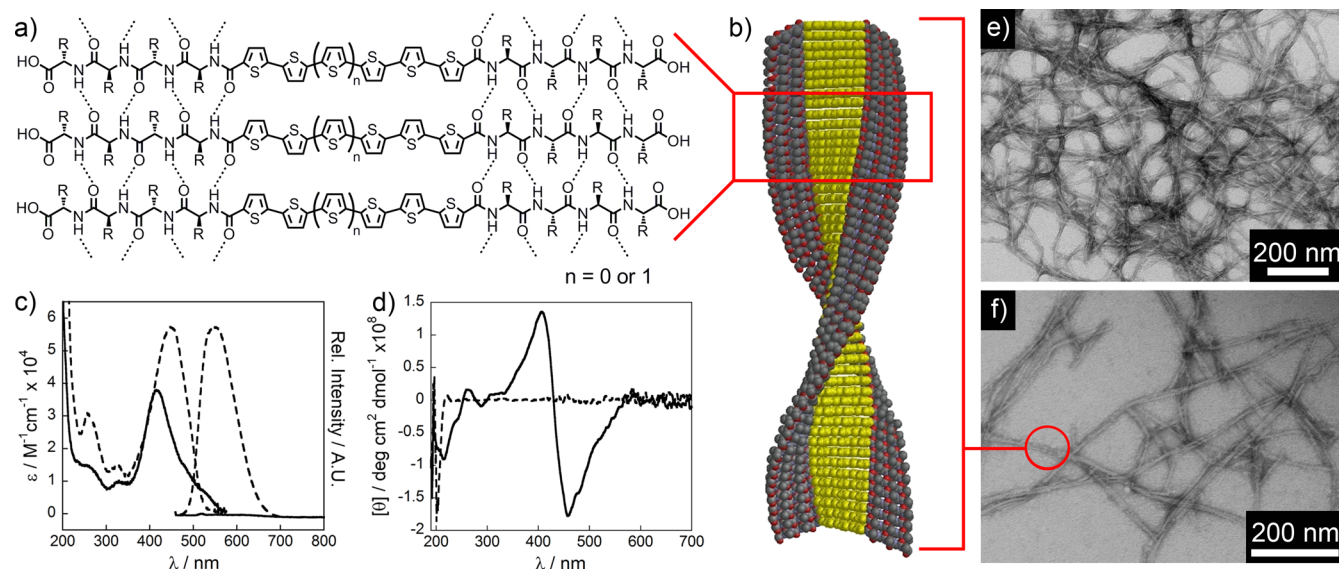


Figure 2. (a) Illustration of a β -sheet network and (b) space-filling model illustrating nanostructures formed from assembly of a generic oligothiophene peptide; UV-vis and photoluminescence (c) and CD spectra (d) of **4** in acidic (assembled, solid line) and basic (unassembled, dashed line) water; TEM images of nanostructures of **3** showing an extensive network (e) and solitary structures (f, diameter: 6–8 nm, molecule in most extended conformation: 4.9 nm).

increasing conjugation length of the embedded oligothiophene subunit with minimal complications from scattering.

Intermolecular self-assembly is expected to occur via favorable hydrogen bonding (Figure 2a,b) to create networks of π -stacking among the embedded chromophores. The exciton coupling among the electronic transition dipoles of these π -electron units in an H-like fashion has been established.^{3b,c,4} However, it is conceivable that longer π -conjugated oligomers here might have less enthalpically favored cofacial π -stacking. More significant quadrupole repulsions between longer conjugated oligomers could potentially drive assembly into a slip-stack type of orientation with less cofacial overlap, competing with the formation of hydrogen bonding networks among the peptide scaffolds. Absorption and photoluminescence data were acquired for all peptides in both their unassembled (pH 8) and assembled (pH 6) states in order to assess these electronic interactions. Upon self-assembly, all peptides displayed a blue shift in the absorption and quenching of the photoluminescence, indicative of H-like aggregation of the chromophore subunits.⁷ The data shown for **4** (Figure 2c) under basic (dashed lines) and acidic (solid lines) conditions is representative. Upon self-assembly, **4** displays a 32 nm blue shift in the λ_{\max} and almost complete quenching of photoluminescence. Circular dichroism spectra were also obtained for each peptide, and the spectra from **4** are shown in Figure 2d. Similar to typical peptidic molecules of this sort, **4** showed no meaningful absorption when in basic solution. Acidic, self-assembled samples of the peptides showed characteristic bisignate Cotton effects, where the ellipticity is zero at the λ_{\max} (415 nm) of the assembled peptide. This suggests that the transition dipoles of the chromophore subunits embedded in the peptides interact via exciton coupling within the chiral environment imposed by tertiary structure when the molecules are assembled, in a manner that remains consistent with H-like aggregation despite the greater quadrupole influence.

TEM imaging was used to characterize nanostructure morphologies (Figure 2e,f). 1-D nanostructure assemblies of **3** on the order of micrometers in length were observed,

comparable to those seen from peptides with less complex π -electron units.³ TEM images of **4** also revealed nanostructures, although smaller in comparison (on the order of hundreds of nanometers in length, Figure S45). The shorter length may be due to the highly charged peptide sequence chosen to maintain solubility or due to enhanced quadrupole repulsions between conjugated oligomeric subunits. Future studies will aim to increase the length of sexithiophene-containing peptide nanostructures and more generally to understand how the interplay of conjugated oligomer length and oligopeptide length influence nanostructure morphology. AFM was also used to investigate the nanostructures of **3** (as a representative example), which supported TEM data. Height profiles of solitary structures in AFM micrographs were found to be between 2 and 5 nm in height. Micrographs and height profiles are shown in Figures S46–S49.

To demonstrate the electrical properties available through the inclusion of longer oligothiophene oligomers within peptide backbones, the nanostructures of sexithiophene **4** were incorporated as the active layer of a field effect transistor. A solution of **4** was dropcast atop a SiO₂ substrate and assembled by treatment with HCl vapor. After drying, gold electrodes were evaporated. Figure 3a depicts the current–

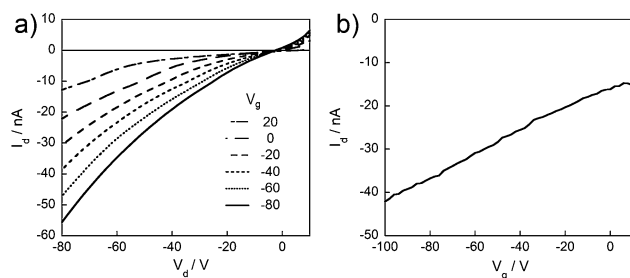


Figure 3. Current–voltage response plots of a field-effect transistor of **4** (a) at gate voltages of 20 V to –80 V, with varied applied drain voltage and (b) at an applied drain voltage of –80 V, with varied applied gate voltage.

voltage output of the transistor at applied gate voltages of 20 to -80 V. The hole mobility of the nanostructures of **4** was found to be $3.8 \times 10^{-5} \text{ cm}^2 \text{ V}^{-1} \text{ s}^{-1}$ by fitting the transfer curve (Figure 3b) data to the linear equation for transistor current. The mobility shows that positive charges can be transported throughout the networks of self-assembled nanostructures. Due to the polycrystallinity of the dropcast film, evident under a light microscope (Figure S1), and the significant amount of insulating side chains, which can increase resistance in the sample, the magnitude of the mobility should not be expected to scale with those of high quality, crystalline organic semiconductors. Peptide-based electronic materials have been subjected to solid-state electrical measurements.^{2b,3e,8} Although it is not appropriate to compare mobilities between devices fabricated with different architectures and protocols, the mobility above is much higher than that for other peptide FETs.

To conclude, we have developed a solid-phase palladium-catalyzed cross-coupling dimerization method in conjunction with standard SPPS. The method grants access to π -conjugated peptides by utilizing soluble, small components, most of which are commercially available, to synthesize π -electron oligomer units on the solid phase. The procedure has allowed for the formation of a diverse array of complex optoelectronic peptide architectures, including the longest aqueous self-assembling oligothiophene-containing system to date. The notorious insolubilities of long π -conjugated oligomeric subunits, such as quinque- and sexithiophene, which previously complicated synthetic work, are no longer an issue for this peptide synthesis, and once incorporated in a peptide backbone, these extended systems are water-soluble and easily manipulated. Each peptide, including the novel sexithiophene **4**, displayed spectral features indicative of H-like aggregation when self-assembly was triggered. Nanostructures of the longer oligothiophene-containing systems (**2–4**) were visualized under TEM, although **4** displayed a lower aspect ratio. Furthermore, a dropcast film of assembled **4**, incorporated into a field effect transistor, displayed a hole mobility of $3.8 \times 10^{-5} \text{ cm}^2 \text{ V}^{-1} \text{ s}^{-1}$. The combination of tunable electronic structures, substantial conductance, and ability to self-assemble under aqueous conditions highlights the prospects for these peptide materials to be viable for future bioelectronic study.

■ ASSOCIATED CONTENT

■ Supporting Information

Experimental, characterization, instrumental details, and additional UV-vis, CD, AFM, and TEM images. This material is available free of charge via the Internet at <http://pubs.acs.org>.

■ AUTHOR INFORMATION

■ Corresponding Author

*E-mail: tovar@jhu.edu.

■ Notes

The authors declare no competing financial interest.

■ ACKNOWLEDGMENTS

We thank Dr. J. Michael McCaffery (JHU IIC), Dr. Cathy Moore, and Mr. Brian Wall for instrumental assistance and Dr. Stephen Diegelmann for early synthetic efforts. T.J.D thanks the JHU Applied Physics Laboratory for a fellowship. We thank Johns Hopkins University and the Department of Energy Office of Basic Energy Sciences (DE-SC0004857, J.D.T. peptide

nanomaterials; DE-FG02-07ER46465, H.E.K. transistor data interpretation) for generous support.

■ REFERENCES

- (1) (a) Ashkenasy, N.; Horne, W. S.; Ghadiri, M. R. *Small* **2006**, *2*, 99–102. (b) Krieg, E.; Shirman, E.; Weissman, H.; Shimani, E.; Wolf, S. G.; Pinkas, I.; Rybtchinski, B. *J. Am. Chem. Soc.* **2009**, *131*, 14365–14373. (c) Chen, L.; Revel, S.; Morris, K.; Adams, D. J. *Chem. Commun.* **2010**, *46*, 4267–4269. (d) Shao, H.; Parquette, J. R. *Chem. Commun.* **2010**, *46*, 4285–4287. (e) Sun, Y.; He, C.; Sun, K.; Li, Y.; Dong, H.; Wang, Z.; Li, Z. *Langmuir* **2011**, *27*, 11364–11371. (f) Tian, L.; Szilluweit, R.; Marty, R.; Bertschi, L.; Zerson, M.; Spitzner, E.-C.; Magerle, R.; Frauenrath, H. *Chem. Sci.* **2012**, *3*, 1512–1521.
- (2) (a) Kas, O. Y.; Charati, M. B.; Rothberg, L. J.; Galvin, M. E.; Kiick, K. L. *J. Mater. Chem.* **2008**, *18*, 3847–3854. (b) Kumar, R. J.; MacDonald, J. M.; Singh, T. M.; Waddington, L. J.; Holmes, A. B. *J. Am. Chem. Soc.* **2011**, *133*, 8564–8573.
- (3) (a) Diegelmann, S. R.; Gorham, J. M.; Tovar, J. D. *J. Am. Chem. Soc.* **2008**, *130*, 13840–13841. (b) Schillinger, E.-K.; Mena-Osteritz, E.; Hentschel, J.; Börner, H. G.; Bäuerle, P. *Adv. Mater.* **2009**, *21*, 1562–1567. (c) Stone, D. A.; Hsu, L.; Stupp, S. I. *Soft Matter* **2009**, *5*, 1990–1993. (d) Shaytan, A. K.; Schillinger, E.-K.; Khalatur, P. G.; Mena-Osteritz, E.; Hentschel, J.; Börner, H. G.; Bäuerle, P.; Khokhlov, A. R. *ACS Nano* **2011**, *5*, 6894–6909. (e) Wall, B. D.; Diegelmann, S. R.; Zhang, S.; Dawidczyk, T. J.; Wilson, W. L.; Katz, H. E.; Mao, H.-Q.; Tovar, J. D. *Adv. Mater.* **2011**, *23*, 5009–5014. (f) Mba, M.; Moretto, A.; Armelao, L.; Crisma, M.; Toniolo, C.; Maggini, M. *Chem.—Eur. J.* **2011**, *17*, 2044–2047.
- (4) Vadehra, G. S.; Wall, B. D.; Diegelmann, S. R.; Tovar, J. D. *Chem. Commun.* **2010**, *46*, 3947–3949.
- (5) (a) Deshpande, M. S. *Tetrahedron Lett.* **1994**, *35*, 5613–5614. (b) Malenfant, P. R. L.; Fréchet, J. M. J. *Chem. Commun.* **1998**, 2657–2658. (c) Conde-Frieboes, K.; Andersen, S.; Breinholt, J. *Tetrahedron Lett.* **2000**, *41*, 9153–9156. (d) Blackwell, H. E.; Clemons, P. A.; Schreiber, S. L. *Org. Lett.* **2001**, *3*, 1185–1188. (e) Bräse, S.; Kirchhoff, J. H.; Köbberling, J. *Tetrahedron* **2003**, *59*, 885–939. (f) Liao, Y.; Fathi, R.; Yang, Z. *J. Comb. Chem.* **2003**, *5*, 79–81. (g) Liao, Y.; Fathi, R.; Yang, Z. *Org. Lett.* **2003**, *5*, 909–912. (h) Doan, N.-D.; Bourgault, S.; Létourneau, M.; Fournier, A. *J. Comb. Chem.* **2008**, *10*, 44–51. (i) Testero, S. A.; Mata, E. G. *J. Comb. Chem.* **2008**, *10*, 487–497. (j) Le Quement, S. T.; Ishoey, M.; Petersen, M. T.; Thastrup, J.; Hagel, G.; Nielsen, T. E. *ACS Comb. Sci.* **2011**, *13*, 667–675.
- (6) Luo, F.; Pan, C.; Wang, W.; Ye, Z.; Cheng, J. *Tetrahedron* **2010**, *66*, 1399.
- (7) Kasha, M.; Rawls, H. R.; Ashraf El-Bayoumi, M. *Pure Appl. Chem.* **1965**, *11*, 371.
- (8) Sun, Y.; Jiang, L.; Schuermann, K. C.; Adriaens, W.; Zhang, L.; Boey, F. Y. C.; De Cola, L.; Brunsveld, L.; Chen, X. *Chem.—Eur. J.* **2011**, *17*, 4746–4749.